References

[1] Selkoe DJ, Schenk D. Alzheimer's disease: molecular understanding predicts amyloid-based therapeutics. Annu Rev Pharmacol Toxicol 2003;43:545–84.
[2] Spillantini MG, Schmidt ML, Lee VM, Trojanowski JQ, Jakes R, Goedert M. α-Synuclein in Lewy bodies. Nature 1997;388:839–40.
[3] Wijesekera LC, Leigh PN. Amyotrophic lateral sclerosis. Orphanet J Rare Dis 2009;4:3.
[4] Zoghbi HY, Orr HT. Glutamine repeats and neurodegeneration. Annu Rev Neurosci 2000;23:217–47.
[5] Soto C. Unfolding the role of protein misfolding in neurodegenerative diseases. Nat Rev Neurosci 2003;4:49–60.
[6] Hoozemans JJ, van Haastert ES, Eikelenboom P, de Vos RA, Rozemuller JM, Scheper W. Activation of unfolded protein response in Parkinson's disease. Biochem Biophys Res Commun 2007;354:707–11.
[7] Hoozemans JJ, van Haastert ES, Nijiholt D, Rozemuller AJ, Eikelenboom P, Scheper W. The unfolded protein response is activated in pretangle neurons in Alzheimer's disease hippocampus. Am J Pathol 2009;174:1241–51.
[8] Katayama T, Imaizumi K, Manabe T, Hitomi J, Kudo T, Tohyama M. Induction of neuronal death by ER stress in Alzheimer's disease. J Chem Neuroanat 2004;28: 67–78.
[9] Lindersson E, Lundvig D, Petersen C, Madsen P, Nyengaard JR, Højrup P, et al. p25α stimulates α-synuclein aggregation and is co-localized with aggregated α-synuclein in α-synucleinopathies. J Biol Chem 2005;280:5703–15.
[10] Rao RV, Bredesen DE. Misfolded proteins, endoplasmic reticulum stress and neurodegeneration. Curr Opin Cell Biol 2004;16:653–62.
[11] Schröder M, Kaufman RJ. ER stress and the unfolded protein response. Mutat Res 2005;569:29–63.
[12] Cooper AA, Gitler AD, Cashikar A, Haynes CM, Hill KJ, Bhullar B, et al. α-Synuclein blocks ER-Golgi traffic and Rab1 rescues neuron loss in Parkinson's models. Science 2006;313:324–8.
[13] Smith WW, Jiang H, Pei Z, Tanaka Y, Morita H, Sawa A, et al. Endoplasmic reticulum stress and mitochondrial cell death pathways mediate A53T mutant α-synuclein-induced toxicity. Hum Mol Genet 2005;14:3801–11.
[14] Stefanova N, Bücke P, Duerr S, Wenning GK. Multiple system atrophy: an update. Lancet Neurol 2009;8:1172–8.
[15] Nakazato Y, Yamazaki H, Hirato J, Ishida Y, Yamaguchi H. Oligodendroglial microtubular tangles in olivopontocerebellar atrophy. J Neuropathol Exp Neurol 1990;49:521–30.
[16] Papp MI, Lantos PL. The distribution of oligodendroglial inclusions in multiple system atrophy and its relevance to clinical symptomatology. Brain 1994;117: 235–43.
[17] Papp MI, Kahn JE, Lantos PL. Glial cytoplasmic inclusions in the CNS of patients with multiple system atrophy (striatonigral degeneration, olivopontocerebellar atrophy and Shy–Drager syndrome). J Neurol Sci 1989;94:79–100.
[18] Arima K, Uéda K, Sunohara N, Arakawa K, Hirai S, Nakamura M, et al. NACP/α-synuclein immunoreactivity in fibrillary components of neuronal and oligodendroglial cytoplasmic inclusions in the pontine nuclei in multiple system atrophy. Acta Neuropathol 1998;96:439–44.
[19] Gai WP, Power JH, Blumbergs PC, Blessing WW. Multiple-system atrophy: a new α-synuclein disease? Lancet 1998;352:547–8.
[20] Tu PH, Galvin JE, Baba M, Giasson B, Tomita T, Leight S, et al. Glial cytoplasmic inclusions in white matter oligodendrocytes of multiple system atrophy brains contain insoluble α-synuclein. Ann Neurol 1998;44:415–22.
[21] Wakabayashi K, Yoshimoto M, Tsuji S, Takahashi H. α-Synuclein immunoreactivity in glial cytoplasmic inclusions in multiple system atrophy. Neurosci Lett 1998;249:180–2.
[22] Southwood CM, Garbern J, Jiang W, Gow A. The unfolded protein response modulates disease severity in Pelizaeus–Merzbacher disease. Neuron 2002;36: 585–96.
[23] Unterberger U, Höftberger R, Gelpi E, Flicker H, Budka H, Voigtländer T. Endoplasmic reticulum stress features are prominent in Alzheimer disease but not in prion diseases in vivo. J Neuropathol Exp Neurol 2006;65:348–57.
[24] Song YJ, Lundvig DM, Huang Y, Gai WP, Blumbergs PC, Højrup P, et al. p25α relocalizes in oligodendroglia from myelin to cytoplasmic inclusions in multiple system atrophy. Am J Pathol 2007;171:1291–303.
[25] Arai N, Nishimura M, Oda M, Morimatsu Y, Oue R. Immunohistochemical study of glial cytoplasmic inclusion in multiple system atrophy. No To Shinkei 1991;43: 857–62.
[26] Conner JR, Fine RE. The distribution of transferrin immunoreactivity in the rat central nervous system. Brain Res 1986;368:319–28.
[27] Yokoo H, Nobusawa S, Takebayashi H, Ikenaka K, Isoda K, Kamiya M, et al. Anti-human Olig2 antibody as a useful immunohistochemical marker of normal oligodendrocytes and gliomas. Am J Pathol 2004;164:1717–25.
[28] Oh D, Prayson RA. Evaluation of epithelial and keratin markers in glioblastoma multiforme: an immunohistochemical study. Arch Pathol Lab Med 1999;123: 917–20.
[29] Sugeno N, Takeda A, Hasegawa T, Kobayashi M, Kikuchi A, Mori F, et al. Serine 129 phosphorylation of α-synuclein induces unfolded protein response-mediated cell death. J Biol Chem 2008;283:23179–88.
[30] Okamoto K, Hirai S, Iizuka T, Yanagisawa T, Watanabe M. Reexamination of granulovacuolar degeneration. Acta Neuropathol 1991;82:340–5.
[31] Takeda A, Arai N, Komori T, Kato S, Oda M. Neuronal inclusions in the dentate fascia in patients with multiple system atrophy. Neurosci Lett 1997;227:157–60.
[32] Bondareff W, Wischik CM, Novak M, Roth M. Sequestration of tau by granulovacuolar degeneration in Alzheimer's disease. Am J Pathol 1991;139: 641–7.
[33] Kadokura A, Yamazaki T, Kakuda S, Makioka K, Lemere CA, Fujita Y, et al. Phosphorylation-dependent TDP-43 antibody detects intraneuronal dot-like structures showing morphological characters of granulovacuolar degeneration. Neurosci Lett 2009;463:87–92.
[34] Leroy K, Boutajangout A, Authelet M, Woodgett JR, Anderton BH, Brion JP. The active form of glycogen synthase kinase-3β is associated with granulovacuolar degeneration in neurons in Alzheimer's disease. Acta Neuropathol 2002;103:91–9.
[35] Chalmers KA, Love S. Neurofibrillary tangles may interfere with Smad 2/3 signaling in neurons. Neuropathol Exp Neurol 2007;66:158–67.
[36] Probst A, Herzig MC, Mistl C, Ipsen S, Tolnay M. Perisomatic granules (non-plaque dystrophic dendrites) of hippocampal CA1 neurons in Alzheimer's disease and Pick's disease: a lesion distinct from granulovacuolar degeneration. Acta Neuropathol 2001;102:636–44.
[37] Wenning GK, Stefanova N, Jellinger KA, Poewe W, Schlossmacher MG. Multiple system atrophy: a primary oligodendrogliopathy. Ann Neurol 2008;64:239–46.
[38] Bloch B, Popovici T, Levin MJ, Tuil D, Kahn A. Transferrin gene expression visualized in oligodendrocytes of the rat brain by using in situ hybridization and immunohistochemistry. Proc Nat Acad Sci USA 1985;82:6706–10.
[39] Abe H, Yagishita S, Amano N, Iwabuchi K, Hasegawa K, Kowa K. Argyrophilic glial intracytoplasmic inclusions in multiple system atrophy: immunocytochemical and ultrastructural study. Acta Neuropathol 1992;84:273–7.
[40] Sakamoto M, Uchihara T, Nakamura A, Mizutani T, Mizusawa H. Progressive accumulation of ubiquitin and disappearance of α-synuclein epitope in multiple system atrophy-associated glial cytoplasmic inclusions: triple fluorescence study combined with Gallyas–Braak method. Acta Neuropathol 2005;110:417–25.
[41] Zhang K, Kaufman RJ. The unfolded protein response: a stress signaling pathway critical for health and disease. Neurology 2006;66:S102–9.
[42] Bail MJ, Lo P. Granulovacuolar degeneration in aging brain and in dementia. J Neuropathol Exp Neuro 1977;l(36):474–87.
[43] Simchowicz T. Histologische Studien fiber die senile Demenz. Histogische und Histopathologische Arbeiten tiber die Grosshirnrinde 1911;4:267–444.
[44] Tomlinson BE, Kitchener D. Granulovacuolar degeneration of hippocampal pyramidal cells. J Pathol 1972;106:165–85.
[45] Woodard JS. Clinicopathologic significance of granulovacuolar degeneration in Alzheimer's disease. J Neuropathol Exp Neurol 1962;21:85–91.
[46] Lee MK, Cleveland DW. Neuronal intermediate filaments. Annu Rev Neurosci 1996;19:187–217.
[47] Kegel KB, Kim M, Sapp E, McIntyre C, Castaño JG, Aronin N, et al. Huntingtin expression stimulates endosomal–lysosomal activity, endosome tubulation, and autophagy. J Neurosci 2000;20:7268–78.
[48] Nixon RA, Wegiel J, Kumar A, Yu WH, Peterhoff C, Cataldo A, et al. Extensive involvement of autophagy in Alzheimer disease: an immuno-electron microscopy study. J Neuropathol Exp Neurol 2005;64:113–22.
[49] Yu WH, Cuervo AM, Kumar A, Peterhoff CM, Schmidt SD, Lee JH, et al. Macroautophagy—a novel β-amyloid peptide-generating pathway activated in Alzheimer's disease. J Cell Biol 2005;171:87–98.
[50] Ogata M, Hino S, Saito A, Morikawa K, Kondo S, Kanemoto S, et al. Autophagy is activated for cell survival after endoplasmic reticulum stress. Mol Cell Biol 2006;26:9220–31.
[51] Yorimitsu T, Klionsky DJ. Endoplasmic reticulum stress: a new pathway to induce autophagy. Autophagy 2007;3:160–2.

International Journal of Neuroscience, 120, 168–175, 2010

ISSN: 0020-7454 print / 1543-5245 online
DOI: 10.3109/00207450903139689

informa
healthcare

Transforming Growth Factor β2 Level is Elevated in Neurons of Alzheimer's Disease Brains

Atsushi Noguchi,[1] Mikiro Nawa,[1] Sadakazu Aiso,[2] Koichi Okamoto,[3] and Masaaki Matsuoka[1]

[1]*Department of Cell Biology and Neuroscience and Department of Anatomy, KEIO University School of Medicine, Shinjuku-ku, Tokyo, Japan*

[2]*Department of Anatomy, KEIO University School of Medicine, Shinjuku-ku, Tokyo, Japan*

[3]*Department of Neurology, Gunma University Graduate School of Medicine, Maebashi, Gunma, Japan*

ABSTRACT

Our earlier studies in vitro indicated that expression of TGFβ2 was induced by toxic amyloid βs (Aβs) in both glial and neuronal cells and increased levels of TGFβ2 triggered a neuronal cell death pathway related to Alzheimer's disease (AD) by binding to the extracellular domain of amyloid β precursor protein (APP). In this study we have demonstrated by immunohistochemical analysis that the levels of TGFβ2 are elevated in cells mainly consisting of neurons of both the hippocampi and cerebral cortices of human AD brains. This result indicates that upregulation of the TGFβ2 level is a common pathological feature of AD brains and suggests that it may be closely linked to the development of neuronal death related to AD.

KEYWORDS: Alzheimer's disease, neuronal death, TGFβ2

INTRODUCTION

Transforming growth factor βs (TGFβs) consisting of three isoforms, TGFβ1, TGFβ2, and TGFβ3, have been shown to be involved in various biological processes (Böttner, Krieglstein, & Unsicker, 2000; Massagué, Blain, & Lo, 2000). They may be proapoptotic or prosurvival in a context-dependent manner. For example, TGFβs play a neuronal-cell-death-inducing role in some situations while they exert neurotrophic function in other situations (Krieglstein, Suter-Crazzolara, Fischer, & Unsicker, 1995; Krieglstein et al., 2000; Mattson, 2000; Poulson et al., 1994).

It has been long assumed that TGFβs may be involved in the pathomechanism of neurodegenerative diseases including Alzheimer's disease (AD). We showed that TGFβ2 promoted neuronal cell death by binding to the extracellular domain of amyloid β precursor protein (APP) in vitro (Hashimoto et al., 2005). Neuronal and glial expression of TGFβ2 was induced by amyloid β (Aβ) (Hashimoto et al., 2006) and anti-TGFβ2 neutralizing antibody inhibited Aβ42-induced death of PCNs (Hashimoto et al., 2006). These results support the notion that TGFβ2 is a neuronal-cell-death-inducing ligand for APP. In accordance, we also demonstrated that expression of TGFβ2 in both neuronal and glial cells was in vitro induced by toxic Aβs and that TGFβ2 expression is generally upregulated in cerebral cortices of mice, in which the Swedish-type familial AD (FAD) gene is constitutively overexpressed and generation of Aβs is markedly upregulated (Hashimoto et al., 2006). In agreement, an immunohistochemical study indicated that expression levels of TGFβ2 were increased in glial cells, especially those surrounding amyloid plaques, and in neurons in the frontal cortex of human samples from FAD brains with presenilin I mutants (Flanders, Lippa, Smith, Pollen, & Sporn, 1995). In addition, the concentrations of TGFβ2 were shown to be upregulated in sera and

We are indebted to Dr. Ikuo Nishimoto for all of this research. We especially thank Ms. Takako Hiraki for essential assistance. This work was supported in part by grants from the Program for Promotion of Fundamental Studies in Health Sciences of the National Institute of Biomedical Innovation (NIBIO).

Address correspondence to Masaaki Matsuoka, Department of Cell Biology and Neuroscience and Department of Anatomy, KEIO University School of Medicine, 35 Shinanomachi, Shinjuku-ku, Tokyo, 160-8582, Japan. E-mail: sakimatu@sc.itc.keio.ac.jp

cerebrospinal fluids of AD patients (Chao et al., 1994). Despite these foregoing studies, however, it remains undetermined whether the TGFβ2 level is commonly upregulated in sporadic AD cases as well as FAD.

In this study, we have demonstrated that TGFβ2 level is significantly elevated in neurons in both the hippocampi and cerebral cortices of sporadic AD brains. This result supports the notion that the upregulation of the TGFβ2 level is a common pathological feature of AD and suggests that it may be closely linked to the development of neuronal loss related AD.

MATERIALS AND METHODS

Vectors

Human TGFβ2 cDNA was obtained by polymerase chain reaction amplification using primers (sense, 5′-GGAATTCACCATGCACTACTGTGTGCTG-3′, and antisense, 5′-CGGGATCCGCTGCATTTGC AAGACTTTACAATC-3′) from human cDNA AD brain frontal lobe (obtained from Biochain Institute Inc.). Subsequently, human TGFβ2 cDNA was subcloned in pCMV-FLAG-5, a vector.

Antibodies

Rabbit TGFβ2 polyclonal antibody was purchased from Santa Cruz Biotech (Santa Cruz, CA). FLAG (M2) monoclonal antibody was purchased from Sigma. Antibody to human tau was from Dako.

Immunohistochemical analysis of human samples

Cerebral cortices and hippocampi used in this study originated from samples of sporadic AD patients, patients with sporadic amyotrophic lateral sclerosis (ALS), and non-AD and non-ALS patients with no pathologic findings in their cerebrums. The ages of AD, ALS, and control groups were 55–97 years (mean, 75.9 ± 13.4 years), 60–79 years (mean, 66.7 ± 6.8 years), and 66–88 years (mean, 77.7 ± 8.0 years), respectively. All AD patients were clinically diagnosed as advanced AD (stage 7 by Functional Assessment Staging Test and stage 3 by Clinical Dementia Rating Scale) and the diagnosis was confirmed by neuropathological analysis at autopsy. Brains of ALS cases that are considered to be normal except for motor neurons were used as another negative control. All ALS cases were not complicated with frontotemporal lobar degeneration. Brain weights of AD cases were 965–1165 g (mean, 1050 g) while those of normal controls and ALS cases were 1050–1330 g (mean, 1120 g) and 1145–1360 g (mean, 1260 g) at autopsy.

Formalin-fixed, paraffin-embedded 5-μm-thick hippocampal and cortical sections were then subjected to neuropathological examination. Sliced sections were deparaffinized, rehydrated to phosphate-buffered saline (PBS), and unmasked in Antigen Unmasking Solution (Vector Laboratories) at 70°C for 10 min. Subsequently, the sections were incubated at room temperature for 20 min in a blocking solution containing normal goat serum in PBS, and then incubated at 4°C over seven nights with anti-TGFβ2 antibody (1:50) or anti-human tau antibody (1:30000).

Immunoreactivity was visualized with three different methods. The first method was by using diaminobenzidine (DAB) after signal amplification with Vectastain Elite ABC kit (Vector Laboratories), mounted on slides, and coverslipped with Entellan new (MERCK, Germany) (the DAB method). The second method was by using the streptoavidin–biotin method (Histofine SAB-PO kit; Nichirei, Tokyo, Japan). The third method was by using Tyramide-FITC (TSA kit; NEN-Perkin-Elmer) (the FITC method). For fluorescent Nissl co-staining, sections were finally incubated with NeuroTrace 530/615 red fluorescent Nissl stain (1:50; Molecular Probes) at room temperature for 30 min and then washed with PBS.

Fluorescence-labeled samples were observed with a laser scanning, confocal microscope LSM 510 (Carl Zeiss, Germany). Fluorescence images were analyzed by Image J 1.37 v.

Quantification of TGFβ2 immunofluorescence intensities of cells

Using Image J 1.37 v, we quantified mean immunofluorescence intensity per pixel of a Nissl-positive and neuron-like morphologic cell (a) and mean immunofluorescence intensity per pixel of a noncell area around the cell (b). Then a ratio of (a) to (b) was calculated as the relative mean immunofluorescence intensity of the cell. Relative mean immunofluorescence intensities of all neuronal cells in 10 random fields of hippocampal CA regions or cortices per sample was calculated for each sample, as shown in the Result section and in Table 1.

Autofluorescence analysis of AD and control brains

To detect the autofluorescence levels, we performed laser microscopical scanning of unstained deparaffinized neighbor samples under the same condition

TABLE 1. Lists of samples and TGFβ2 immunofluorescence intensities

	Age/Sex	Brain weight (g)	Tissue	TGFβ2 level	Tissue	TGFβ2 level
Normal	71/F	1330	Hippocampus	2.69	Parietal lobe	3.16
	79/F	1150	Hippocampus	6.84	Occipital lobe	6.98
	83/M	1050	Hippocampus	4.62	Parietal lobe	4.20
	88/M	1100	Hippocampus	4.52	Parietal lobe	6.40
	66/M	1240	Hippocampus	3.65	Parietal lobe	4.87
	79/M	1310	Hippocampus	4.38	Parietal lobe	5.27
	64/F	1290	Hippocampus	3.49	Occipital lobe	3.10
	69/F	1145	Hippocampus	4.08	Occipital lobe	2.66
	60/M	1290	Hippocampus	3.32	Occipital lobe	4.44
ALS	79/M	1360	Hippocampus	3.67	Occipital lobe	3.31
	62/M	1300	Hippocampus	4.46	Occipital lobe	5.64
	66/M	1150	Hippocampus	3.89	Occipital lobe	7.26
	55/F	965	Hippocampus	8.89	Occipital lobe	7.92
	79/F	1080	Hippocampus	13.41	Occipital lobe	16.50
	65/M	1090	Hippocampus	NE	Occipital lobe	16.46
AD	73/M	1050	Hippocampus	8.87	Parietal lobe	18.31
	79/F	1050	Hippocampus	10.52	Parietal lobe	13.69
	83/F	1165	Hippocampus	6.73	Parietal lobe	13.54
	97/F	1060	Hippocampus	8.30	Occipital lobe	17.64

Note: Hippocampal sections and sections of outer pyramidal layers and inner pyramidal layers of parietal or occipital lobes from AD patients, ALS patients, and controls were immunostained with antibody to TGFβ2. Immunodetection was performed with the FITC method. Relative mean immunofluorescence intensities (TGFβ2 levels) were measured with Image J 1.37 v, as described in detail in the Materials and Methods section. NE indicates "not examined" because of poor fixation state. Ten microscopical areas were randomly selected per sample. Average relative mean immunofluorescence intensity of all Nissl-positive and neuron-like cells in the 10 areas was calculated for each sample.

as used for the detection of each TGFβ2-stained sample.

Cell cultures

COS7 cells were grown in Dulbecco's modified Eagle's medium (DMEM) supplemented with 10% FBS and 2 mM glutamine. Transient transfection was performed with lipofectAMINE PLUS™ reagents according to the manufacturer's instructions (Gibco-BRL, MD), as shown previously.

Immunocytochemistry

COS7 cells seeded on a coverslip at a density of 3.0×10^4 were transfected with C-terminally FLAG-tagged TGFβ2 encoding vectors. At 48 hr after transfection, they were fixed with 4% paraformaldehyde in PBS for 24 hr at 4°C, rinsed two times with PBS, permeabilized with 0.1% Triton X-100 in PBS for 3 min, blocked for 5 min with 0.1% BSA in PBS at room temperature, and then stained with the TGFβ2 antibody (1:200) for 60 min at room temperature. Subsequently, they were stained with the FLAG (M2) antibody (1:200) for 60 min at room temperature. After being washed three times with 0.1% BSA in PBS, cells were stained with FITC-conjugated goat anti-rabbit IgG (1:250) (Jackson ImmunoResearch Laboratories, West Grove, PA) or Texas-Red-conjugated goat anti-mouse IgG (1:250) (Jackson ImmunoResearch Laboratories, West Grove, PA) for 60 min at room temperature. Before detection, they were washed three times with 0.1% BSA in PBS. Fluorescence signals were detected with a laser scanning, confocal microscope LSM (Carl Zeiss, Germany).

In an experiment, the antibody was preincubated with or without immunizing peptide whose amount was 25-fold (by weight) more than the amount of antibody in PBS with 0.1% BSA under constant rotation at 4°C for 24 hr before immunostaining of COS7 cells.

Statistical analyses

Values in the figures are mean ± SE. Statistical analysis was carried out by the one way-ANOVA followed by a post hoc test (Fisher's PLSD test). $p < .001$ were assessed as significant.

RESULTS

Specific recognition of TGFβ2 by an antibody to TGFβ2

To test the specificity of the TGFβ2 antibody, we ectopically overexpressed FLAG-tagged TGFβ2 in COS7 cells by transfection. As shown in Figure 1(A), COS cells overexpressing TGFβ2–FLAG were immunocytochemically stained by the anti-TGFβ2 antibody as well as anti-FLAG antibody while those

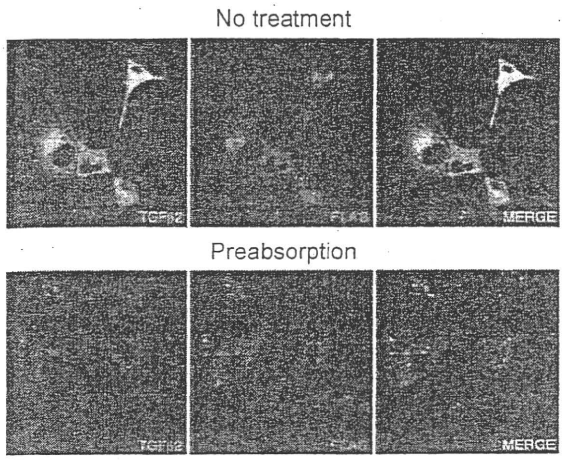

FIGURE 1 Characterization of TGFβ2 antibody. TGFβ2 antibody specifically recognized TGFβ2. (A and B) COS7 cells were transfected with the TGFβ2–FLAG-encoding vector. At 48 hr after transfection, cells were fixed and stained with □ indicated antibodies or Hoechst. (B) The TGFβ2 antibody was preincubated with/without immunizing peptide whose amount was 25-fold (by weight) more than the amount of antibody under constant rotation in PBS with 0.1% BSA at 4°C for 24 hr and the antibody/peptide mixture was then used for immunostaining. Hoechst 33258 (indicated Hoechst) was used for staining of nucleus.

not overexpressing TGFβ2–FLAG were not stained by either antibody (stained only with Hoechst 33258). In Figure 1(B), both the anti-TGFβ2 and anti-FLAG antibodies immunocytochemically recognized TGFβ2–FLAG overexpressed in COS7 cells (top panel). However, preincubation of the TGFβ2 antibody with the immunizing peptide markedly reduced immunoreactivity of cells to TGFβ2, but not immunoreactivity of cells to FLAG (bottom panel). These results indicated that the TGFβ2 antibody specifically recognized TGFβ2.

TGFβ2 level is upregulated in the hippocampal and neocortical cells of AD brains

We examined whether TGFβ2 expression is upregulated in hippocampi and cerebral cortices of AD brains. All AD cases were clinically diagnosed as advanced AD (stage 7 by Functional Assessment Staging Test and stage 3 by Clinical Dementia Rating Scale). Immunohistochemical analysis also confirmed that there were many typical neurofibrillary tangles (Figure 2) and senile plaques (data not shown) in hippocampi and cortices of all AD cases while there were few neurofibrillary tangles and senile plaques in control cases. First of all, hippocampi of an AD case (81 years old, female) and a non-AD

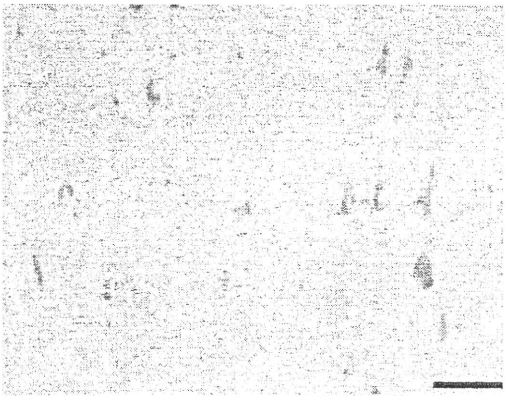

FIGURE 2 Detection of neurofibrillar tangles in AD hippocampus. A hippocampal section (pyramidal layers of the CA1 regions from an AD patient (79 years old, female) was immunostained with antibody to tau. Immunodetection was performed with the streptoavidin–biotin method. Scale bars, 50 μm.

(normal) case (76 years old, female) were immunostained with the anti-TGFβ2 antibody and visualized by the DAB method (Figure 3). Anatomically similar hippocampal regions (the pyramidal cell layers of the

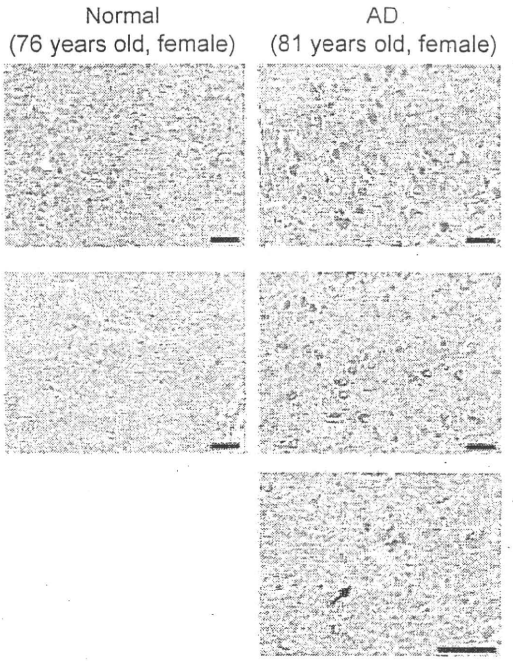

FIGURE 3 Elevated TGFβ2 level in the AD hippocampal neurons (DAB method). Hippocampal sections (pyramidal layers of the CA1 regions (left panels) and CA4 regions (right panels)) from an AD patient (81 years old, female) and a control (76 years old, female) were immunostained with antibody to TGFβ2. A senile plaque is shown in the middle of CA1 region of the hippocampal section of the AD patient (arrow). Immunodetection was performed with the DAB method. To strengthen the TGFβ2 signal. Scale bars, 50 μm.

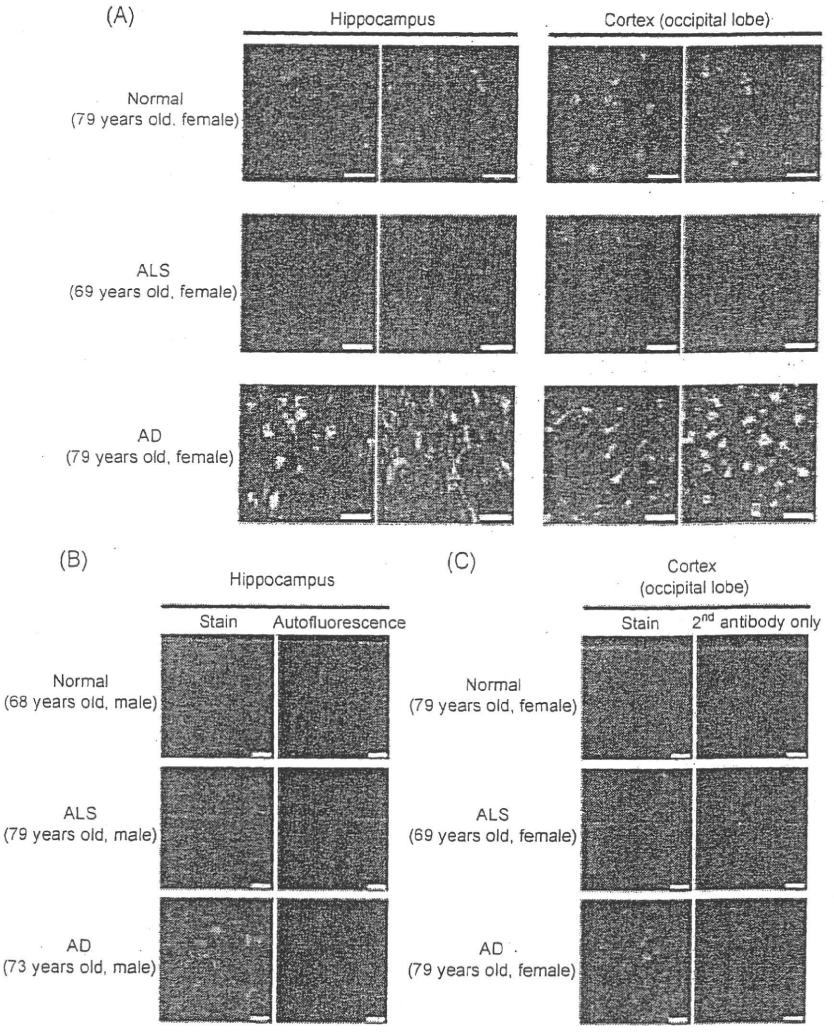

FIGURE 4 Elevated TGFβ2 levels in neurons of the AD hippocampus and cortex (FITC method). (A) Hippocampal sections (pyramidal layers of the CA1 regions (left panels) and CA4 regions (right panels)) and two sections of outer pyramidal layers and inner pyramidal layers of occipital lobes from an AD patient (79 years old, female), an ALS patient (69 years old, female), and a control (79 years old, female) were immunostained with antibody to TGFβ2. Immunodetection was performed with the FITC method. Fluorescent Nissl co-staining was performed to recognize all cells contained in the fields. Scale bars, 50 μm. (B) Autofluorescence of unstained hippocampal sections (pyramidal layers of the CA4 region) from an AD patient (73 years old, male), an ALS patient (79 years old, male), and a control (88 years old, male) were examined under the same condition as used for the detection of TGFβ2-immunostained neighbor samples. TGFβ2 immunodetection was performed with the FITC method, as shown in (A). Scale bars, 50 μm. (C) Neighbor cortical sections from an AD patient (79 years old, female), an ALS patient (69 years old, female), and a control (79 years old, female) were immunostained with or without TGFβ2 antibody (stain or 2nd antibody only). Immunodetection was performed with the FITC method, as shown in (A). Scale bars, 50 μm.

CA1 and CA4 regions) were immunostained. Note a senile plaque in another CA1 region of hippocampus of the same AD patient (the right panel of the AD patient). The TGFβ2 levels in hippocampal cells in the pyramidal layer of these regions mainly consisting of neurons (and/or glial cells) were generally elevated as compared with those of the normal brain.

To confirm the elevated TGFβ2 levels of AD brains as compared with those of normal controls, we further performed immunohistochemical analysis using the FITC method. Fluorescent Nissl co-staining was performed to recognize all cells contained in the fields. As shown in Figure 4(A), the TGFβ2 level was elevated in hippocampal neuronal cells of an AD

brain (79 years old, female) as compared with those of normal (non-AD, non-ALS) brains (79 years old, female). We simultaneously stained brain samples from ALS patients as controls because ALS is a selective motoneuronal disease and found that the TGFβ2 level was not significantly elevated in hippocampal cells of an ALS brain (69 years old, female). The TGFβ2 level was also elevated in outer pyramidal cells and inner pyramidal cells mainly consisting of neurons in occipital lobes of cerebral cortices of the AD brain as compared with those of the normal and ALS brains (Figure 4A, right panels).

To exclude the possibility that the elevation of TGFβ2 levels incidentally occurred in a single AD case, we examined six or five other AD, ALS, and aged normal brains by the FITC method. We then found that TGFβ2 levels were elevated in hippocampal and cortical neuronal cells of all examined AD brains as compared with those of ALS or normal brains (data not shown but see parts of these immunofluorescence pictures in Figures 4B and C).

Elevation of TGFβ2 levels was not caused by cellular autofluorescence

It has been reported that autofluorescence increased in aged neurons mainly due to increased intracellular lipofuscin (Van de Lest, Versteeg, Veerkamp, & Van Kuppevelt, 1995). Such autofluorescence may contribute to the increase in TGFβ2 immunofluorescence levels. To exclude this possibility, we examined cellular autofluorescence in an unstained continuous neighbor brain sample under the same condition of the laser microscopy as used for the immunofluorescence detection of each TGFβ2-stained sample (Figure 4B). As shown in Figure 4(B), autofluorescence was not detected under the same condition. We also performed immunostaining of another continuous neighbor brain sample only with second antibody as a negative control and found that significant immunofluorescence was not detected under the same condition as used for the immunofluorescence detection of each TGFβ2-stained sample (Figure 4C). These results supported our notion that the TGFβ2 level was elevated in hippocampal and cortical neuronal cells of the AD brains.

Quantification of elevated TGFβ2 levels in AD brains

To quantify cellular TGFβ2 levels, we examined mean cytoplasmic immunofluorescence intensity per pixel of a Nissl-positive and neuron-like morphologic cell (a), as shown in Figure 5(A). We simultaneously quantified mean immunofluorescence intensity per pixel of a noncell area around the cell (b). Then a ratio of (a) to (b) was calculated as a relative mean immunofluorescence intensity of the cell. We randomly selected 10 microscopical areas in each sample, and fluorescence intensities of all neuronal cells were measured and an average relative mean immunofluorescence intensity was calculated for each sample, as shown in Table 1. Statistical analysis indicated that the TGFβ2 level was significantly elevated in cells mainly consisting of neurons of the hippocampi and cortices of AD brains (Figure 5B) (Table 1).

DISCUSSION

We have herein demonstrated that the TGFβ2 level is upregulated in cells mainly consisting of neurons in hippocampi and cortices of sporadic AD brains. This result is consistent with our earlier in vitro data (Hashimoto et al., 2006) as well as a foregoing in vivo study which indicated that TGFβ2 levels in autopsied FAD cases with presenilin 1 mutations were upregulated in reactive glial cells around senile plaques and neurons with neurofibrillary tangles (Flanders et al., 1995). In addition to normal aged brains, we examined the hippocampi and cortices of brains of ALS cases without frontotemporal lobar degeneration which are thought to be completely normal (except for cortices containing motor neurons) (Figure 4). As expected, levels of TGFβ2 were not increased in normal and ALS brains. Thus, this study contributes to the establishment of the notion that the upregulation of the neuronal TGFβ2 level is a common pathological feature of AD.

We showed that Aβ42 increased the intracellular TGFβ2 level (Hashimoto et al., 2006). However, in the current experiment, the intracellular TGFβ2 levels around senile plaques are not significantly higher than those not around senile plaques (data not shown). This result suggests that there are other important mechanisms than the upregulation of Aβ42 underlying the increase in the TGFβ2 level in AD brains.

In earlier studies, it was hypothesized that TGFβ2 might behave as a mediator of defensive reaction and the neuronal and glial levels of TGFβ2 were upregulated so that neurons survive in neurological diseases including AD (Krieglstein et al., 1995), based on the fact that the levels of TGFβ2 were increased in the surviving neurons and the speculation that neurons without upregulation of the TGFβ2 level died. However, there is no direct evidence supporting the notion that upregulated TGFβ2 inhibits neuronal cell death in AD brains. Conversely, based on the experimental findings showing that TGFβ2 promotes neuronal

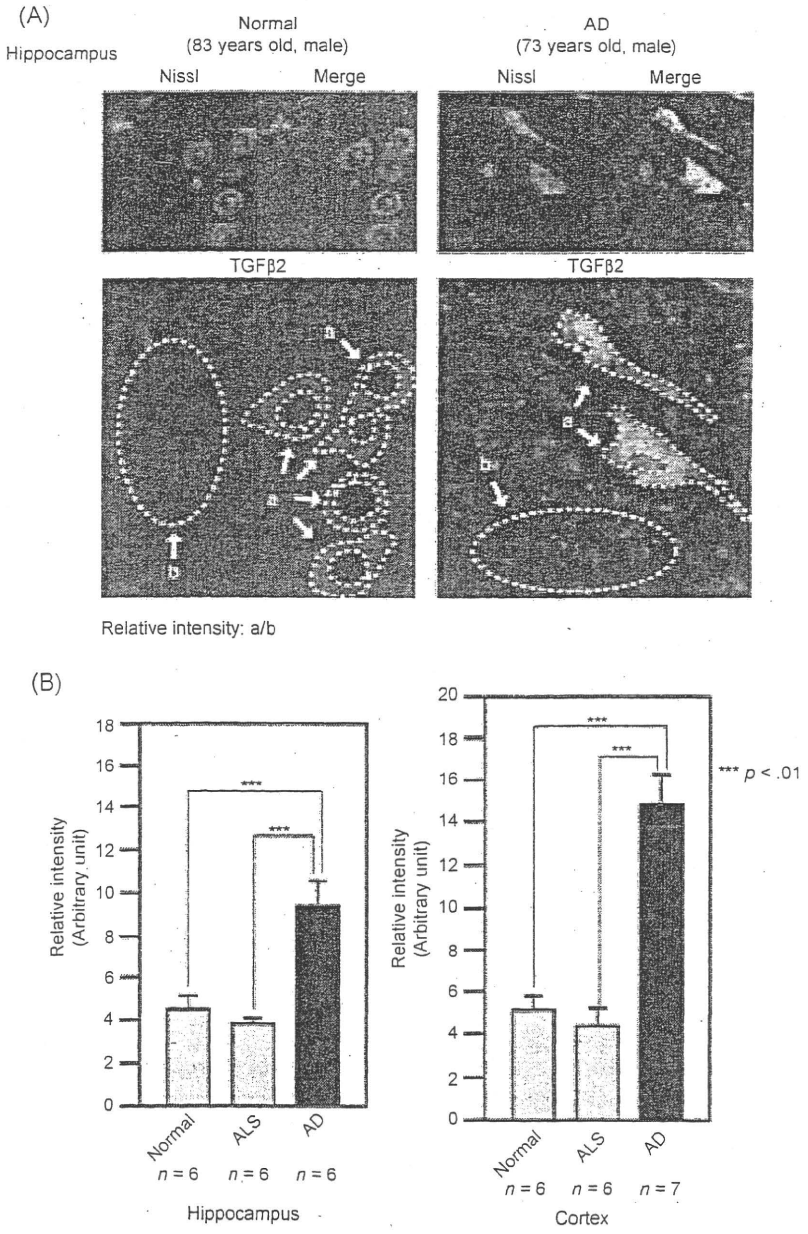

FIGURE 5 Quantification of the elevated levels of neuronal TGFβ2. (A) Two examples of quantification of cellular immunofluorescence intensity are demonstrated. A Nissl-positive and neuron-like morphologic cell area (a) and a noncell area surrounding the cell (b) were enclosed by marking and mean immunofluorescence intensity per pixel were measured for each area. Then a ratio of (a) to (b) was calculated as the relative mean immunofluorescence intensity of the neuron. (B) Hippocampal sections and cortex (parietal or occipital lobes not containing motor neurons) from AD patients, ALS patients, and normal controls shown in Table 1 (including those shown in (A)) were immunostained with antibody to TGFβ2. Immunodetection was performed with the FITC method. Mean immunofluorescence intensities were measured with Image J 1.37 v, as described in detail in the Materials and Methods section. Data are shown as mean ± SEM.

cell death by binding to the extracellular domain of APP in vitro (Hashimoto et al., 2005), neuronal and glial expressions of TGFβ2 were induced by Aβ (Hashimoto et al., 2006), and anti-TGFβ2 neutralizing antibody inhibited Aβ42-induced death of PCNs (Hashimoto et al., 2006), it could be alternatively speculated that upregulated TGFβ2 promotes neuronal cell death in vivo, and neurons generating

relatively lower levels of TGFβ2 or neurons with more self-defensive ability may survive in brains of human AD cases. It is also possible that the elevated TGFB signal in neurons is a simple secondary effect of AD and is not related to the AD pathogenesis.

One of the hallmarks of the human AD pathology is neuronal loss (Hardy & Selkoe, 2002; Mattson, 2000). Neuronal loss is directly linked to the catastrophic and irreversible dementia, while neuronal dysfunction is linked to the reversible dementia of AD. Although it is speculated in the Aβ cascade hypothesis that long exposure of neurons to increased levels of Aβs ultimately results in neuronal cell death (Hardy & Selkoe, 2002), the detailed molecular mechanism underlying this process remains undetermined. This study reinforces the hypothesis proposed by a series of the foregoing studies that upregulated TGFβ2 may be a mediator of this process (Hashimoto et al., 2005, 2006; Matsuoka, Hashimoto, Aiso, & Nishimoto, 2006). Further investigation is needed to ultimately differentiate whether TGFβ2 is neurotoxic or neurotrophic in AD or whether the upregulation of TGFβ2 is a simple secondary effect unrelated to the AD pathogenesis.

Declaration of Interest: We have no conflicts of interests.

REFERENCES

Böttner, M., Krieglstein, K., & Unsicker, K. (2000). The transforming growth factor-βs: Structure, signaling, and roles in nervous system development and functions. *Journal of Neurochemistry, 75*, 2227–2240.

Chao, C. C., Hu, S., Frey, W. H., Ala, T. A., Tourtellotte, W. W., & Peterson, P. K. (1994). Transforming growth factor β in Alzheimer's disease. *Clinical and Diagnostic Laboratory Immunology, 1*, 109–110.

Flanders, K. C., Lippa, C. F., Smith, T. W., Pollen, D. A., & Sporn, M. B. (1995). Altered expression of transforming growth factor-beta in Alzheimer's disease. *Neurology, 45*, 1561–1569.

Hardy, J., & Selkoe, D. J. (2002). The amyloid hypothesis of Alzheimer's disease: Progress and problems on the road to therapeutics. *Science, 297*, 353–356.

Hashimoto, Y., Chiba, T., Yamada, M., Nawa, M., Kanekura, K., Suzuki, H., et al. (2005). Transforming growth factor beta2 is a neuronal cell death-inducing ligand for amyloid-β precursor protein. *Molecular and Cell Biology, 25*, 9304–9317.

Hashimoto, Y., Nawa, M., Chiba, T., Aiso, S., Nishimoto, I., & Matsuoka, M. (2006). Transforming growth factor beta2 autocrinally mediates neuronal cell death induced by amyloid-beta. *Journal of Neuroscience Research, 83*, 1039–1047.

Krieglstein, K., Richter, S., Farkas, L., Schuster, N., Dunker, N., Oppenheim, R. W., et al. (2000). Reduction of endogenous transforming growth factors β prevents ontogenetic neuron death. *Nature Neuroscience, 3*, 1085–1090.

Krieglstein, K., Suter-Crazzolara, C., Fischer, W. H., & Unsicker, K. (1995). TGF-β superfamily members promote survival of midbrain dopaminergic neurons and protect them against MPP + toxicity. *EMBO Journal, 14*, 736–742.

Massagué, J., Blain, S. W., & Lo, R. S. (2000). TGFβ signaling in growth control, cancer, and heritable disorders. *Cell, 103*, 295–309.

Matsuoka, M., Hashimoto, Y., Aiso, S., & Nishimoto, I. (2006). Humanin and Colivelin: Neuronal-death-suppressing peptides for Alzheimer's disease and ALS. *CNS Drug Reviews, 12*, 113–122.

Mattson, M. P. (2000). Apoptosis in neurodegenerative disorders. *Nature Reviews Molecular Cell Biology, 1*, 120–130.

Poulson, K. T., Armanini, M. P., Klein, R. D., Hynes, M. A., Phillips, H. S., Rosenthal, A. (1994). TGF-β2 and TGF-β3 are potent survival factors for midbrain dopaminergic neurons. *Neuron, 13*, 1245–1252.

Schuster, N., & Krieglstein, K. (2000). Mechanisms of TGF-β-mediated apoptosis. *Cell and Tissue Research, 307*, 1–14.

Van de Lest, C. H., Versteeg, E. M., Veerkamp, J. H., & Van Kuppevelt. (1995). Elimination of autofluorescence in immunofluorescence microscopy with digital image processing. *Journal of Histochemistry and Cytochemistry, 43*, 727–730.

NEUROPATHOLOGY

Neuropathology 2011; **31**, 42–47 doi:10.1111/j.1440-1789.2010.01123.x

Original Article

Morphological changes of Golgi apparatus in adult rats after facial nerve injuries

Yukio Fujita,[1] Kazuhiko Watabe,[2] Ken Ikeda,[3] Yuji Mizuno[1] and Koichi Okamoto[1]

[1]Department of Neurology, Gunma University Graduate School of Medicine, Gunma, [2]Department of Molecular Neuropathology, Tokyo Metropolitan Institute for Neuroscience, and [3]Department of Neurology, Toho University Omori Medical Center, Tokyo, Japan

We examined the morphological changes of Golgi apparatus (GA) of the facial motor neurons in rats after facial nerve avulsion or axotomy. In rats after avulsion, the numbers of motor neurons showed reduction and fragmentation of GA, namely the organelle lost the normal network-like configuration which was replaced by numerous small disconnected elements (fine fragmentation). This GA fragmentation was morphologically indistinguishable from that previously reported in amyotrophic lateral sclerosis (ALS). On the other hand, axotomy did not induce significant motor neuron loss, and the GA had lost the elongated profiles (coarse fragmentation). These results suggest that there may be a similar cascade leading to motor neuron death in rats after avulsion, and ALS and GA observed in rats after axotomy may not be related to neuronal death.

Key words: amyotrophic lateral sclerosis, avulsion, axotomy, facial nerve, Golgi apparatus.

INTRODUCTION

As animal models of motor neuron degeneration, there are rats that have undergone avulsion or axotomy of peripheral nerves.[1–5] Significant neuronal degeneration is observed in both neonatal and adult rats after avulsion; however, the neuronal degeneration seen in adult rats after axotomy is generally milder compared to that in neonatal rats. The precise mechanisms behind these differences are not known. On the other hand, several reports showed that the fragmentation of Golgi apparatus (GA), namely the organelle, lost the normal network-like configuration which was replaced by numerous small disconnected elements (fine fragmentation), and was frequently observed in the motor neurons of patients with amyotrophic lateral sclerosis (ALS) and mice expressing G93A mutation of the *SOD1* gene, before the first signs of clinical dysfunction.[6–10] These results strongly suggest that the GA is an early target of the pathological processes initiating neuronal degeneration in ALS. We herein investigated using immunohistological methods whether the fragmented GA of the facial motor neurons is also present in rats after facial nerve avulsion or axotomy. If fine fragmentation of the GA is present, it is reasonable to propose that there may be a similar cascade leading to motor neuron death in rats with injured facial nerve and ALS.

MATERIALS AND METHODS

The experimental protocols were approved by the Animal Care and Use Committee of the Tokyo Metropolitan Institute for Neuroscience. Eighteen adult Fisher 344 male rats (12–14 weeks old, 200–250 g) were prepared for facial nerve axotomy or avulsion, respectively, and then they were anesthetized with an intraperitoneal injection of pentobarbital sodium (40 mg/kg). As for facial nerve avulsion, the right facial nerve was exposed at its exit from the stylomastoid foramen and avulsed by gentle traction as described elsewhere.[3,4] Regarding axotomy, the right facial nerve was transected at its exit from the stylomastoid foramen, and a distal portion of the nerve, 5 mm in length, was cut and removed.[1] After 30 min to 4 weeks, rats were anesthetized with a lethal dose of pentobarbital sodium and transcardially perfused with 0.1 M phosphate buffer (PB), pH 7.4 followed by 4% paraformaldehyde in 0.1 M PB. The brain stem tissues containing facial nuclei were dissected and immersion-fixed in the same fixative for 2 h. The tissues were dehydrated and embedded in paraffin.

Correspondence: Yukio Fujita, MD, Department of Neurology, Gunma University Graduate School of Medicine 3-39-15 Showa-machi, Maebashi, Gunma 371-8511, Japan. Email: yfujita@showa.gunma-u.ac.jp

Received 29 January 2010; revised and accepted 24 March 2010; published online 19 May 2010.

Every fifth section (24-μm intervals) of each 2 rats were collected at 30 min, 2 h, 6 h, 1day, 3 days, 1 week, 2 weeks, 3 weeks and 4 weeks after avulsion or axotomy, respectively. For facial motor neuron cell counting, the sections were deparaffinized, and stained with cresyl violet (Nissl staining), and facial motor neurons having nuclei containing distinct nucleoli were counted in 25 sections as described elsewhere.[3]

Immunohistochemistry

A polyclonal anti-MG-160 antibody (1:700 dilution, gifted by Gonatas NK: University of Pennsylvania School of Medicine, PA, US), which recognizes a sialoglycoprotein of the medial cisternae of the GA, was used to demonstrate the morphological changes of the GA.[11,12] Autoclave treatment (121°C, 10 min) was required to improve antigen retrieval for the anti-MG-160 antibody. The sections were incubated with polyclonal anti-MG-160 antibody overnight at 4°C, followed by a secondary reagent containing biotinylated anti-rabbit IgG for 30 min, and finally labelled streptoavidin-biotin methods for 30 min. The tissues were subjected to peroxidase reaction using diaminobenzidine.

Electron microscopy

For electron microscopy, the tissues were fixed with 3% gultaraldehyde in 0.1M PB, pH 7.4, post-fixed in 4% osmic acid, then embedded in epoxy resin. Ultrathin sections were double-stained with uranyl acetate and lead citrate, and observed with a JEM 200CX electron microscope (JEOL Co., Ltd., Tokyo, Japan).

RESULTS

The numbers of facial motor neurons on the ipsilateral side of rats after avulsion were reduced compared to the contralateral side at 2–4 weeks (Fig. 1B). On the other hand, neurons on the ipsilateral side of rats after axotomy did not show a significant loss (Fig. 1C). The average percentages of surviving facial motor neurons after avulsion reached 20–30% of the contralateral side by 4 weeks (Fig. 2). GA of the motor neurons in rats was adequately and specifically immunostained with the anti-MG-160 antiserum (Fig. 3). GA of the contralateral side in rats after avulsion or axotomy showed a normal profile, being larger, angular, or elongated, and filling the cell body (Fig. 3A). On the other hand, approximately 3%, 28%, 68%, 55% and 34% of the GA in the remaining facial motor neurons on the ipsilateral side showed fine fragmentation in adult rats at 3 days, 1 week, 2 weeks, 3 weeks and 4 weeks after avulsion, respectively (Fig. 3B). In contrast to avulsion, we observed few fine fragmentations of GA in the facial motor neurons in rats after facial nerve axotomy; however, approximately

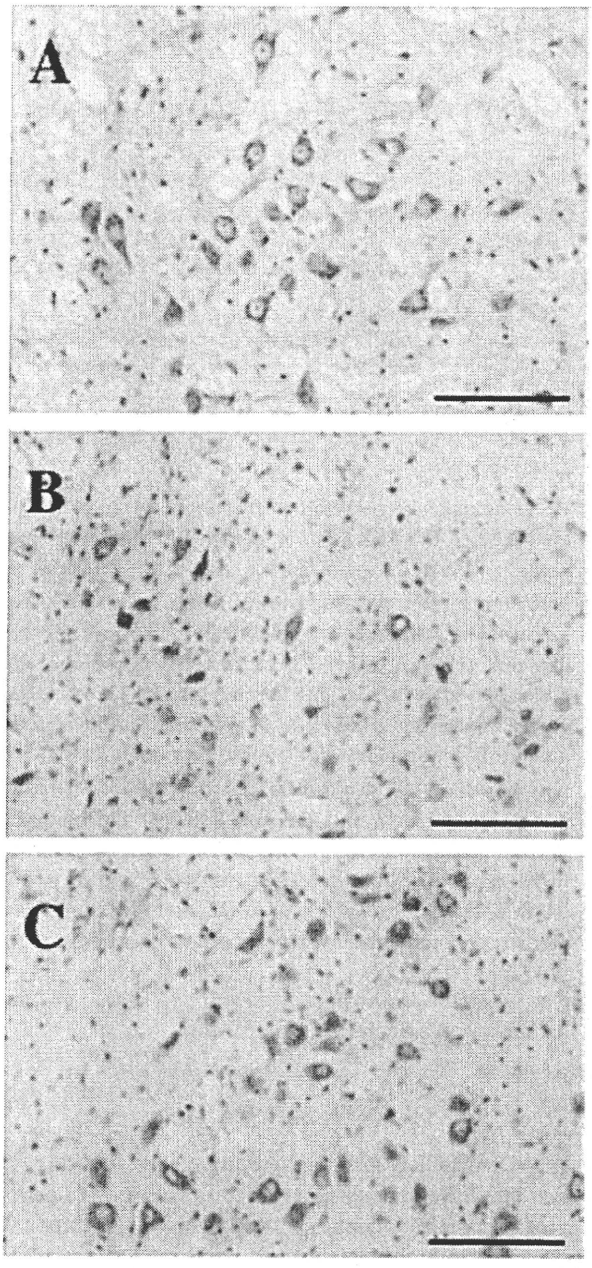

Fig. 1 Facial motor neurons on the contralateral (A) and ipsilateral (B, C) sides 4 weeks after facial nerve avulsion (A, B) and axotomy (C). The surviving facial motor neurons on the ipsilateral side (B) were reduced in number compared with the contralateral side (A) in a rat after avulsion. On the other hand, the number of neurons after facial nerve axotomy did not show a significant reduction (C). Nissl stain. Bar = 100 μm.

34%, 52%, 40% and 34% of the GA in the facial motor neurons on the ipsilateral side at 1–4 weeks showed GA changes which had lost the elongated profiles (coarse fragmentation), respectively (Fig. 3C).

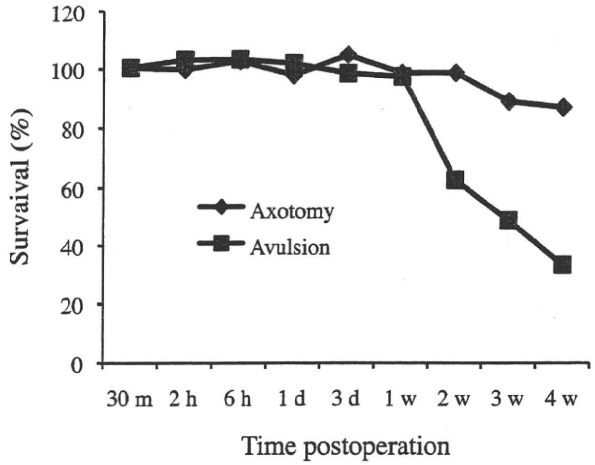

Fig. 2 Time courses of facial motor neuron loss after operations. The average percentages of surviving facial motor neurons in 25 sections of two rats after facial nerve avulsion or axotomy are plotted. m: minutes, h: hours, d: days, w: weeks.

In electron microscopy, GA of the ipsilateral side in rats after both avulsion and axotomy showed short cisternae compared to the contralateral side (Fig. 4), while coated and uncoated vesicles in the vicinity of the residual shortened cisternae of the GA were virtually absent. Further, the arrangements of shorter cisternae in rats after avulsion were more irregular than that in rats after axotomy (Fig. 4B,C).

DISCUSSION

The extent of motor neuron loss after peripheral nerve injury is highly variable. In neonatal rats, axotomy induces the degeneration of motor neurons, and neuronal apoptosis has been shown to be the major mechanism of cell death.[13,14] On the other hand, the neuronal degeneration seen in adult rats after axotomy is generally milder compared to that in neonatal rats, and no neuronal apoptosis is observed.[15,16] In contrast to axotomy, peripheral nerve avulsion induces significant degeneration of motor neurons in both neonatal and adult rats. Martin *et al.* demonstrated motor neuronal apoptosis after sciatic nerve avulsion in adult rats;[2] however, other studies failed to show neuronal apoptosis in both neonatal and adult rats after avulsion.[17] The precise molecular mechanisms behind these differences between avulsion and axotomy are not known; however, the peroxinitrite-mediated oxidative damage and perikaryal accumulation or phosphorylated neurofilaments, both of which were observed in motor neurons in ALS, were also demonstrated in injured motor neurons after avulsion.[2,18-20] Thus, rats with peripheral nerve avulsion are good models of motor neuron degeneration in ALS.

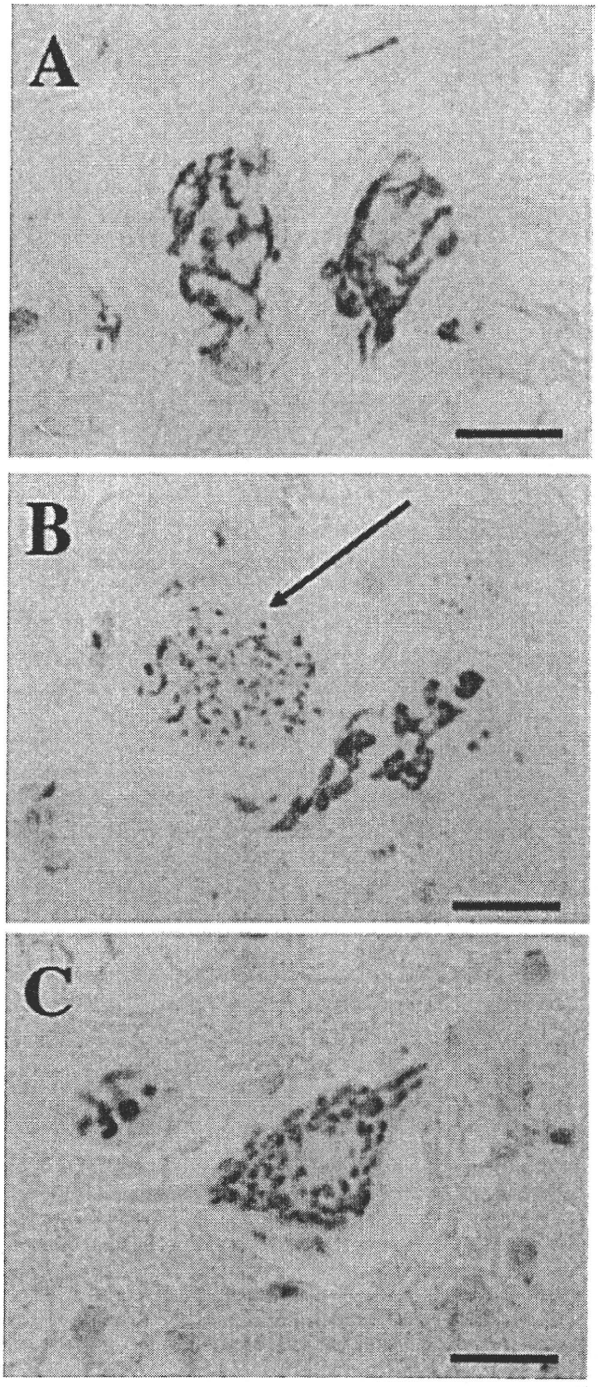

Fig. 3 Immunostaining of the facial motor neurons on the contralateral side in a rat at 4 weeks after avulsion (A), ipsilateral side in a rat at 1 week after avulsion (B) and ipsilateral side in a rat at 2 week after axotomy (C) with anti-MG-160 antibody. A facial motor neuron on the contralateral side showed a normal Golgi apparatus (GA) profile (A). Fine fragmentation of GA was observed in the facial motor neuron of a rat after avulsion (B, arrow), and the GA in the facial motor neuron of a rat after axotomy showed coarse fragmentation (C). Bar = 20 μm.

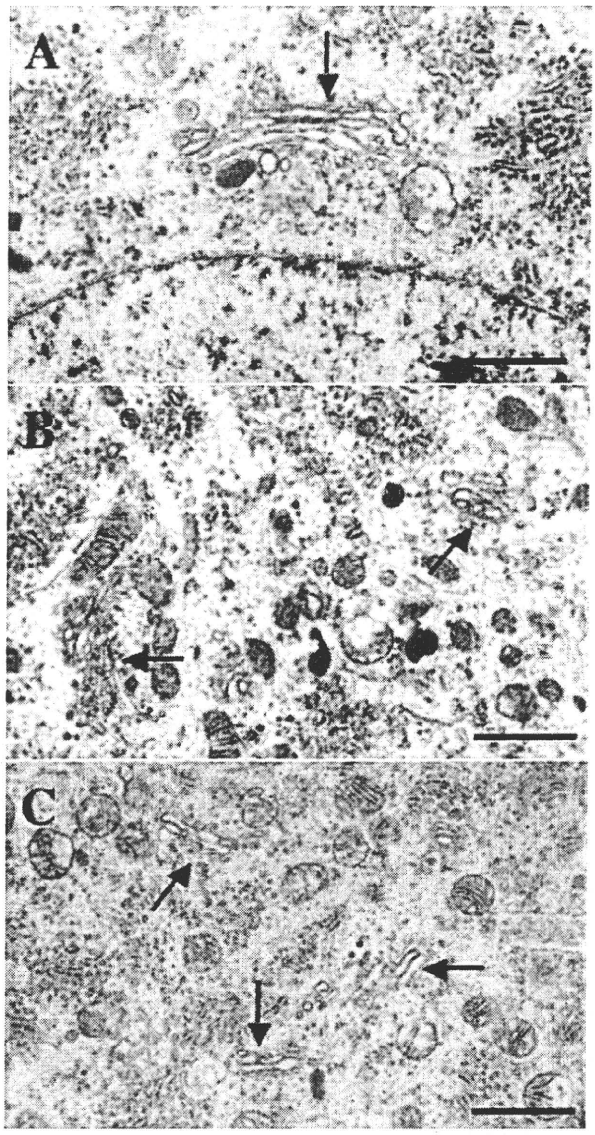

Fig. 4 Electron microscopy of the facial motor neurons on the contralateral side in a rat at 4 weeks after avulsion (A), ipsilateral side in a rat at 4 weeks after avulsion (B), and ipsilateral side in a rat at 4 weeks after axotomy (C). Golgi apparatus of the ipsilateral side in rats after both avulsion and axotomy (B, C, arrows) showed short cisternae compared to the contralateral side (A, arrow), and the arrangements of shorter cisternae in rats after avulsion (B) were more irregular than that in rats after axotomy (C). Bar = 1 μm.

Morphological changes of GA were also described as mildly hypertrophic in the hypoglossal motor neurons of rats at the end of the first week following axotomy;[21] however, these GA changes were not detected in motor neurons in rats after facial nerve avulsion. We demonstrated the frequent fine fragmentation of the GA of motor neurons in rats after facial nerve avulsion. Similar GA fragmentation was frequently observed in motor neurons of the spinal cord and motor cortex in ALS patients, and in transgenic mice expressing human mutant Cu/Zn superoxide dismutase (G93A).[6–10] Of course, fine fragmentation of GA was not specific for ALS;[22,23] however, the GA of motor neurons were more frequently fragmented in patients with ALS than other neurodegenerative diseases and a majority of motor neurons contained cytoplasmic inclusions had fine-fragmented GA.[24] Further, GA fragmentation is one of the early neuropathological changes in transgenic mice expressing the G93A mutation of the *SOD1* gene.[10] These results suggest that fine fragmentation of GA may be related to neuronal degeneration in patients with ALS. Therefore, our results suggest that a similar cascade of motor neuron death may be present in rats with peripheral nerve avulsion and ALS.

On the other hand, fine-fragmented GA of motor neurons was rare on the ipsilateral side of rats after axotomy, and approximately 34–52% of facial motor neurons at 1–4 weeks after axotomy showed coarse fragmentation of the GA. In this study, we demonstrated that axotomized neurons did not show significant loss; therefore, we considered that these morphological changes of the GA observed in rats after axotomy may \ not be related to neuronal death.

The biological difference between axotomy and avulsion has been considered the difference in the length of the remaining axons and whether there are cells such as Schwann cells adjacent to the axons.[25] In contrast to axotomy, avulsion causes the complete disappearance of peripheral nerve components, including Schwann cells, which produce several neuroprotective molecules for motor neurons. A recent study revealed that cytoplasmic RNA content per neuron decreased markedly in the facial nucleus after facial nerve avulsion compared with that after axotomy, and the degree of decrease of cytoplasmic RNA in motor neurons was correlated with the extent of loss of large motor neurons.[25] Therefore, we speculate that the loss of some neuroprotective molecules may induce a disturbance of protein metabolism and cause fine fragmentation of GA.

By electron microscopic study, we demonstrated that GA of the ipsilateral side in rats after both avulsion and axotomy showed short cisternae compared to the contralateral side, while coated and uncoated vesicles in the vicinity of the residual shortened cisternae of the GA were virtually absent. In contrast, in cells undergoing apoptotic cell death, the stacks of the cisternae of the GA are replaced by clusters of vesicles similar to those seen in mitosis.[23,26] Therefore, our results may support that neuronal death in our facial nerve avulsion model was not apoptosis.

Further studies are needed to clarify the significance of GA morphological changes in these animals using immunoelectron microscopy.

ACKNOWLEDGEMENTS

This work was supported by a Grant-in-Aid for Scientific Research (C) to Y. Fujita (21591108), and by grants from the Ministry of Health, Labor and Welfare of Japan and from the Ministry of Education, Culture, Sports, Science and Technology of Japan to K. Okamoto.

REFERENCES

1. Ikeda K, Aoki M, Kawazoe Y *et al.* Motoneuron degeneration after facial nerve avulsion is exacerbated in presymptomatic transgenic rats expressing human mutant Cu/Zn superoxide dismutase. *J Neurosci Res* 2005; **82**: 63–70.
2. Martin LJ, Kaiser A, Price AC. Motor neuron degeneration after sciatic nerve avulsion in adult rat evolves with oxidative stress and is apoptosis. *J Neurobiol* 1999; **40**: 185–201.
3. Sakamoto T, Watabe K, Ohashi T *et al.* Adenoviral vector-mediated GDNF gene transfer prevents death of adult facial motoneurons. *Neuroreport* 2000; **11**: 1857–1860.
4. Sakamoto T, Kawazoe Y, Shen JS *et al.* Adenoviral gene transfer of GDNF, BDNF and TGF 2, but not CTNF, cardiotrophin-1 or IGF1, protects injured adult motoneurons after facial nerve avulsion. *J Neurosci Res* 2003; **72**: 54–64.
5. Watabe K, Hayashi Y, Kawazoe Y. Peripheral nerve avulsion injuries as experimental models for adult motoneuron degeneration. *Neuropathology* 2005; **25**: 371–380.
6. Fujita Y, Okamoto K, Sakurai A, Amari M, Nakazato Y, Gonatas NK. Fragmentation of the Golgi apparatus of Betz cells in patients with amyotrophic lateral sclerosis. *J Neurol Sci* 1999; **163**: 81–85.
7. Fujita Y, Okamoto K. Golgi apparatus of the motor neurons in patients with amyotrophic lateral sclerosis and in mice models of amyotrophic lateral sclerosis. *Neuropathology* 2005; **25**: 388–394.
8. Gonatas NK, Stieber A, Mourelatos Z *et al.* Fragmentation of the Golgi apparatus of motor neurons in amyotrophic lateral sclerosis. *Am J Pathol* 1992; **140**: 731–737.
9. Mourelatos Z, Yachnis A, Rorke L, Mikol J, Gonatas NK. The Golgi apparatus of motor neurons in amyotrophic lateral sclerosis. *Ann Neurol* 1993; **33**: 608–615.
10. Mourelatos Z, Gonatas NK, Stieber A, Gurney ME, Dal Canto MC. The Golgi apparatus of spinal cord motor neurons in transgenic mice expressing mutant Cu,Zn superoxide dismutase (SOD) becomes fragmented in early, preclinical stages of the disease. *Proc Natl Acad Sci USA* 1996; **93**: 5472–5477.
11. Croul S, Mezitis SGE, Stieber A *et al.* Immunocytochemical visualization of the Golgi apparatus in several species, including human, and tissues with an antiserum against MG-160, a sialoglycoprotein of rat Golgi apparatus. *J Histochem Cytochem* 1990; **38**: 957–963.
12. Gonatas JO, Mezitis SGE, Stieber A, Fleischer B, Gonatas NK. MG-160: a novel sialoglycoprotein of the medial cisternae of the Golgi apparatus. *J Biol Chem* 1989; **264**: 646–653.
13. de Bilbao F, Dubois-Dauphin M. Time course of axotomy-induced apoptotic cell death in facial motoneurons of neonatal wild type and bcl-2 transgenic mice. *Neuroscience* 1996; **71**: 1111–1119.
14. Rossiter JP, Riopelle RJ, Bisby MA. Axotomy-induced apoptotic cell death of neonatal rat facial motoneurons: time course analysis and relation to NADPH-diaphorase activity. *Exp Neurol* 1996; **138**: 33–44.
15. Mattsson P, Delfani K, Janson AM, Svensson M. Motor neuronal and glial apoptosis in the adult facial nucleus after intracranial nerve transection. *J Neurosurg* 2006; **104**: 411–418.
16. McPhail LT, Vanderluit JL, McBride CB *et al.* Endogenous expression of inhibitor of apoptosis proteins in facial motoneurons of neonatal and adult rats following axotomy. *Neuroscience* 2003; **117**: 567–575.
17. Li L, Houenou LJ, Wu W, Lei M, Prevette DM, Oppenheim RW. Characterization of spinal motoneuron degeneration following different types of peripheral nerve injury in neonatal and adult mice. *J Comp Neurol* 1998; **396**: 158–168.
18. Cleveland DW. From Charcot to SOD1: mechanisms of selective motor neuron death in ALS. *Neuron* 1999; **24**: 515–520.
19. Cleveland DW, Rothstein JD. From Charcot to Lou Gehrig: deciphering selective motor neuron death in ALS. *Nat Rev Neurosci* 2001; **2**: 806–819.
20. Estévez AG, Spear N, Manuel SM, Barbeito L, Radi R, Beckman JS. Role of endogenous nitric oxide and peroxynitrite formation in the survival and death of motor neurons in culture. *Prog Brain Res* 1998; **118**: 269–280.
21. Flumerfelt BA, Lewis PR. Cholinesterase activity in the hypoglossal nucleus of the rat and the changes produced by axotomy: a light and electron microscopic study. *J Anat* 1975; **119**: 309–331.
22. Fujita Y, Ohama E, Takatama M, Al-Sarraj S, Okamoto K. Golgi apparatus of nigral neurons with α-synuclein-positive inclusions in patients with Parkinson's disease. *Acta Neuropathol* 2006; **112**: 261–265.
23. Gonatas NK, Stieber A, Gonatas JO. Fragmentation of the Golgi apparatus in neurodegenerative diseases and cell death. *J Neurol Sci* 2006; **246**: 21–30.

24. Fujita Y, Mizuno Y, Takatama M, Okamoto K. Anterior horn cells with abnormal TDP-43 immunoreactivities show fragmentation of the Golgi apparatus in ALS. *J Neurol Sci* 2008; **269**: 30–34.
25. Nagasao J, Hayashi Y, Kawazoe Y, Kawakami E, Watabe K, Oyanagi K. Relationship between ribosomal RNA gene transcription activity and motoneuron death: observation of avulsion and axotomy of the facial nerve in rats. *J Neurosci Res* 2008; **86**: 435–442.
26. Sesso A, Fujiwara DT, Jaeger M *et al.* Structual elements common to mitosis and apoptosis. *Tissue Cell* 1999; **31**: 357–371.

NEUROPATHOLOGY

Neuropathology 2010 doi:10.1111/j.1440-1789.2010.01146.x

Case Report

Numerous FUS-positive inclusions in an elderly woman with motor neuron disease

Yukio Fujita,[1] Sayaka Fujita,[2] Masamitsu Takatama,[3] Masaki Ikeda[1] and Koichi Okamoto[1]

[1]Department of Neurology, Gunma University Graduate School of Medicine, Gunma, Departments of [2]Neurology and [3]Internal Medicine, Geriatric Research Institute and Hospital, Gunma, Japan

We report an autopsy case of a 75-year-old Japanese woman with motor neuron disease (MND) showing numerous neuronal and glial inclusions immunostained with anti-fused in sarcoma (FUS) antibody. At 73 years, she received a diagnosis of MND and died of respiratory insufficiency 2 years later. No mutation was found in all exons of the *FUS* gene. Neuropathological examination revealed a reduced number of anterior horn cells and degeneration of the pyramidal tracts. Neither Bunina bodies nor inclusions positive for ubiquitin/phosphorylated TAR DNA binding protein of 43 kD (pTDP-43), such as skein-like or round inclusions, were observed. However, basophilic inclusions (BIs) were frequently observed in the remaining neurons of the anterior horns, facial nuclei, hypoglossal nuclei, vestibular nuclei, dentate nuclei and inferior olivary nuclei. In an immunohistochemical analysis, the BIs showed strong immunoreactivity with anti-FUS and anti-ubiquitin-binding protein p62 (p62) antibodies. The nuclear staining of FUS was preserved in some neurons with FUS-positive inclusions, and a few FUS-positive glial inclusions were found. FUS-positive inclusions were more common than p62-positive inclusions in some anatomical regions, and in some neurons, p62 immunoreactivity was observed in only parts of the BIs. These results suggest that BI formation and TDP-43 aggregation have different pathogenic mechanisms, and FUS may play an important role in the pathogenesis of MND with BIs. This patient has the oldest reported age of onset for MND with BIs, and clinical features observed in this patient were indistinguishable from those of classic sporadic MND. Therefore, we consider that the age of onset and clinical features of FUS-related disorders may be variable.

Correspondence: Yukio Fujita, MD, Department of Neurology, Gunma University Graduate School of Medicine, 3-39-15, Showa-machi, Maebashi, Gunma 371-8511, Japan. Email: yfujita@showa.gunma-u.ac.jp

Received 18 February 2010; revised and accepted 3 June 2010.

Key words: amyotrophic lateral sclerosis, basophilic inclusion, FUS, motor neuron disease, neuropathology.

INTRODUCTION

Amyotrophic lateral sclerosis (ALS) is a chronic degenerative disease characterized by progressive degeneration and loss of motor neurons in the spinal cord, brain stem and motor cortex. The etiology of the sporadic form of ALS, which accounts for approximately 90% of all cases, is unknown. Of all cases of familial ALS (FALS), 15–20% are caused by mutations in the Cu/Zn superoxide dismutase 1 (*SOD1*) gene, and an additional 5–10% are caused by mutations in the TAR DNA binding protein of 43 kD (*TDP-43*) gene.[1] Recently, two studies have implicated mutations in the gene encoding the fused in sarcoma protein (FUS) in the etiology of FALS type 6.[2,3] Furthermore, *FUS* gene mutations have been identified in patients with FALS and sporadic ALS.[4,5] FUS has been also immunohistochemically detected in the inclusions found in neuronal intermediate filament inclusion disease (NIFID) and basophilic inclusion body disease (BIBD).[6,7] BIBD is classified into two subtypes: a generalized variant Pick's disease and a motor neuron disease (MND) characterized by the presence of basophilic inclusions (BIs).[8] MND with BIs was previously referred to as juvenile MND because cases of adult-onset disease were rare.[9–12] Here, we report an autopsy of an elderly woman with MND showing numerous BIs which were strongly immunostained with anti-FUS antibodies in multiple anatomical regions. Furthermore, this patient had no mutations in the *FUS* gene, and the clinical features observed in this patient were indistinguishable from those of classic sporadic MND without apparent pyramidal tract signs.

CLINICAL SUMMARY

The patient was a 75-year-old Japanese woman who noticed weakness in her right hand at the age of 73. Past

medical and family histories were negative for neurological disorders. Neurological examinations revealed progressive muscle weakness and atrophy in the right hand and generalized areflexia. Tongue atrophy and fasciculation, facial weakness, dysarthria, dysphagia, extrapyramidal signs, cognitive dysfunction, cerebellar ataxia and Babinski sign were not observed. Ocular movements, sensation and the autonomic nervous system were also normal. Laboratory tests revealed that the patient's serum creatine kinase level was slightly elevated and the cerebrospinal fluid (CSF) protein level was normal. Computed tomography (CT) scan of the brain revealed mild frontal lobe atrophy, and cervical magnetic resonance imaging (MRI) showed normal results. The findings of nerve conduction studies in the extremities were normal, but needle electromyography revealed acute and chronic neurogenic changes in her upper and lower limbs. Because of progressive muscle weakness, she became bedridden 2 years after the onset of the symptoms. She died of respiratory insufficiency at the age of 75, 2 years and 4 months after the onset of symptoms.

GENE ANALYSIS OF *FUS*

We purified genomic DNA from the brain of this patient. Genomic DNA was extracted from frozen brain samples by using standard methods.[13] The PCR products of *FUS* were generated with intronic primers located upstream from exon 1 to exon 15.[3] The PCR products were excised from a 3% Nusieve (FMC Bioproducts, Rockland, ME, USA) agarose gel, purified, and treated with the T vector cloning system pGEM-T® (PROMEGA, Madison, WI, USA). The plasmid clones were then subjected to sequencing with an ABI 3130XL Genetic Analyzer (Applied Biosystems, Foster City, CA, USA).

NEUROPATHOLOGICAL FINDINGS

Autopsy was performed 2 h after death. The general autopsy findings were unremarkable. The brain (weight = 1000 g) and spinal cord were fixed in phosphate-buffered formalin and embedded in paraffin. Brain and spinal cord sections (thickness = 5 μm) were stained with HE, KB and Gallyas-Braak stains and were immunostained with several antibodies. To compare HE staining with Gallyas-Braak stain and immunostaining in the same sections, some sections were stained with HE, photographed, decolorized using alcohol and PBS, and then stained with Gallyas-Braak silver method and immunostained.

Immunohistochemical analyses

Several deparaffinized sections (thickness = 5 μm) of the brain, brainstem and spinal cord were incubated with 1% H_2O_2 in methanol for 30 min to eliminate endogenous peroxidase activity in the tissue. The sections were blocked with normal serum and incubated overnight at 4°C with the following antibodies: rabbit polyclonal anti-ubiquitin antibody (1:2000; Dako, Glostrup, Denmark), mouse monoclonal anti-phosphorylated neurofilament (pNF) antibody (1:10 000; SMI 31, Sternberger-Meyer, Jarrettsville, MD, USA), rabbit polyclonal anti-phosphorylated TDP-43 (pTDP-43) antibody (1:3000; phosphorylated C-terminal Ser409/410 of the synthetic peptide derived from human TDP-43, CSMDSKS(p)S(p)GWGM),[14] rabbit polyclonal anti-α-synuclein antibody (1:8000; MPVDPDNEAYEMPSEE, a synthetic peptide derived from α-synuclein),[15] mouse monoclonal anti-phosphorylated tau antibody (AT-8, 1:2000; Innogenetics, Ghent, Belgium), mouse monoclonal anti-glial fibrillary astrocyte protein (GFAP) antibody (1:500; Dako), guinea pig monoclonal antibodies against the N-terminals of p62 (1:2000; Progen Biotechnik, Heidelberg, Germany), rabbit polyclonal anti-α-internexin antibody (1:100; Abcam, Cambridge, UK), and rabbit polyclonal anti-FUS antibody (1:500; Sigma, St Louis, MO, USA). Antibodies against pTDP-43 and α-synuclein were prepared in our laboratory.[14,15]

The sections were washed in PBS for 30 min and incubated in biotinylated anti-rabbit, anti-mouse, or anti-guinea pig secondary antibodies for 1 h and then in streptavidin-biotinylated horseradish peroxidase complex (Histofine SAB-PO kit; Nichirei, Tokyo, Japan) for 30 min. The peroxidase labeling was visualized with 3, 3′-diaminobenzidine (DAB) as the chromogen, and the sections were counterstained with hematoxylin. Before the sections were stained with antibodies against pTDP-43, pNF, p62, α-internexin, and FUS, they were treated with 10 mM sodium citrate buffer in an autoclave at 121°C for 10 min.

Immunofluorescence analyses

Double-labelled immunofluorescence was performed on the spinal cord by using a rabbit polyclonal anti-FUS antibody and a guinea pig monoclonal anti-p62 antibody. The secondary antibodies were Alexa Fluor 594-conjugated anti-rabbit (1:100) and Alexa Fluor 488-conjugated anti-guinea pig (1:100) (Molecular Probes–Invitrogen, Eugene, OR, US). 4′-6-diamidino-2-phenylindol (DAPI; Southern Biotech, Birmingham, AL, US) was used for nuclear counterstaining.

ULTRASTRUCTURAL STUDY

The anterior horns from the lumbar spinal cord were fixed with 4% paraformaldehyde and 2% glutaraldehyde in 0.1 mol/L PBS, cut into small pieces, post-fixed in 2%

osmium tetroxide for 2 h, dehydrated and embedded in epoxy resin. The embedded specimens were then cut into semi-thin sections and stained with toluidine blue. The BIs were identified by light microscopy, after which appropriate portions of the specimens were trimmed and cut into ultra-thin sections. These sections were stained with uranyl acetate and lead citrate and examined under a JEM 100CX (JEOL Co., Ltd. Tokyo, Japan) electron microscope.

RESULTS

No mutation was detected in the sequences of all exons in the *FUS* gene of this patient.

Neuropathologically, we observed neuronal loss in the anterior horns and hypoglossal nuclei as well as mild degeneration of the pyramidal tracts. A few spheroids were found in the anterior horns. Bunina bodies and ubiquitin/pTDP-43-positive inclusions, such as skein-like or round inclusions, were not observed in the anterior horn cells. On the other hand, round or globular BIs were frequently observed in the neurons of the anterior horns and in the facial, vestibular, hypoglossal, dentate and inferior olivary nuclei (Fig. 1a1–e1). The BIs were weakly argyrophilic with Gallyas-Braak stain (Fig. 1a2). Immunohistochemical analysis showed that the BIs were negative for pNF, pTDP-43, α-synuclein, phosphorylated-tau, GFAP and α-internexin. A few BIs were weakly stained with anti-ubiquitin antibody but strongly stained with FUS antibody (Fig. 1b2,c2). BIs were also immunostained with anti-p62 antibody, but some BIs labeled only part of the inclusion (Fig. 1d2,e2). Nuclear immunostaining of FUS was preserved in a significant number of the neurons containing BIs (Fig. 2). Furthermore, FUS-positive neuronal inclusions were also present in the neurons of the substantia nigra, oculomotor nuclei, red nuclei, inferior olivary nuclei, facial nuclei, pontine nuclei, dentate nuclei, hypoglossal nuclei, vestibular nuclei and locus coerulei (Fig. 3). A few neuronal FUS-positive inclusions were observed in the thalamus and globus pallidus. Glial cytoplasmic inclusions and dystrophic neurites were observed in the regions where the neuronal FUS-positive inclusions were observed (Fig. 3). No FUS-positive inclusions were observed in the Betz cells and the neurons of the cerebral cortex and the granule cells of the dentate gyrus. Immunofluorescence analysis revealed that all p62-positive BIs were also FUS-positive. On the other hand, some FUS-positive BIs labeled only part of the inclusion for anti-p62 antibody and a few FUS-positive inclusions were negative for anti-p62 antibody (Fig. 4). The Betz cells, Onuf nuclei, Clarke column, Purkinje cells, caudate nuclei, amygdala, putamen and substantia nigra were well preserved. A few neurofibrillary tangles and threads were found in the parahippocampal gyrus and amygdala (Braak stage I) and no Lewy pathology was detected using α-synuclein antibody.

Electron microscopy revealed that the BIs consisted of thick filamentous structures associated with granules. The BIs had no limiting membranes. Rough endoplasmic reticulum was frequently observed on the periphery and mitochondria were enclosed within the inclusions (Fig. 5).

DISCUSSION

We have described the clinical and neuropathological findings from an elderly patient with MND showing numerous BIs. The inclusions observed in this patient were found to be basophilic when stained with HE and KB stains. Immunohistochemical analysis revealed that the BIs were negative for pNF, pTDP-43, α-synuclein, phosphorylated-tau, GFAP and α-internexin antibodies. A few BIs were weakly stained with anti-ubiquitin antibody, but strongly stained with anti-FUS and anti-p62 antibodies. These findings have also been demonstrated in previous reports[6,12,16] and are compatible with BIs observed in patients with BIBD as mentioned in the consensus criteria recently reported by the Consortium for Frontotemporal Lobar Degeneration (FTLD).[17] BIBD is divided into two subtypes: a generalized variant Pick's disease and MND with BIs.[8] The generalized variant Pick's disease is associated with clinical evidence of frontotemporal dementia. Because our patient did not have dementia, we diagnosed her as having MND with BIs.

Recently, the *FUS* gene, located on chromosome 16p11.2, has been implicated in the etiology of FALS type 6.[2,3] This gene encodes a 526-amino acid protein that binds to RNA and is known to be involved in RNA processing. Neuropathological examination has revealed nuclear FUS immunoreactivity in both controls and patients with FALS type 6. Patients who have FALS with *FUS* gene mutations exhibit increased neuronal cytoplasmic FUS immunoreactivity, dystrophic neuritis and globular neuronal cytoplasmic inclusions.[2,3] Recently, Munoz *et al.* immunohistochemically labeled the neuronal inclusions found in BIBD with anti-FUS antibody and concluded that FUS may play an important role in the pathogenesis of this condition.[6] Similarly, we found that the inclusions in this case exhibited strong immunostaining with the anti-FUS antibody. FUS is involved in regulating transcription, RNA splicing, and transport and is functionally homologous to another ALS-related gene, *TDP-43*, which has been identified as a major component of cytoplasmic inclusions in the motor neurons of patients with sporadic MND and FTLD with ubiquitinated inclusions.[18,19] Thus, protein aggregation in the neuronal cytoplasm and defective RNA metabolism may be a mechanism responsible for motor neuron degeneration in both sporadic ALS and MND with BIs.

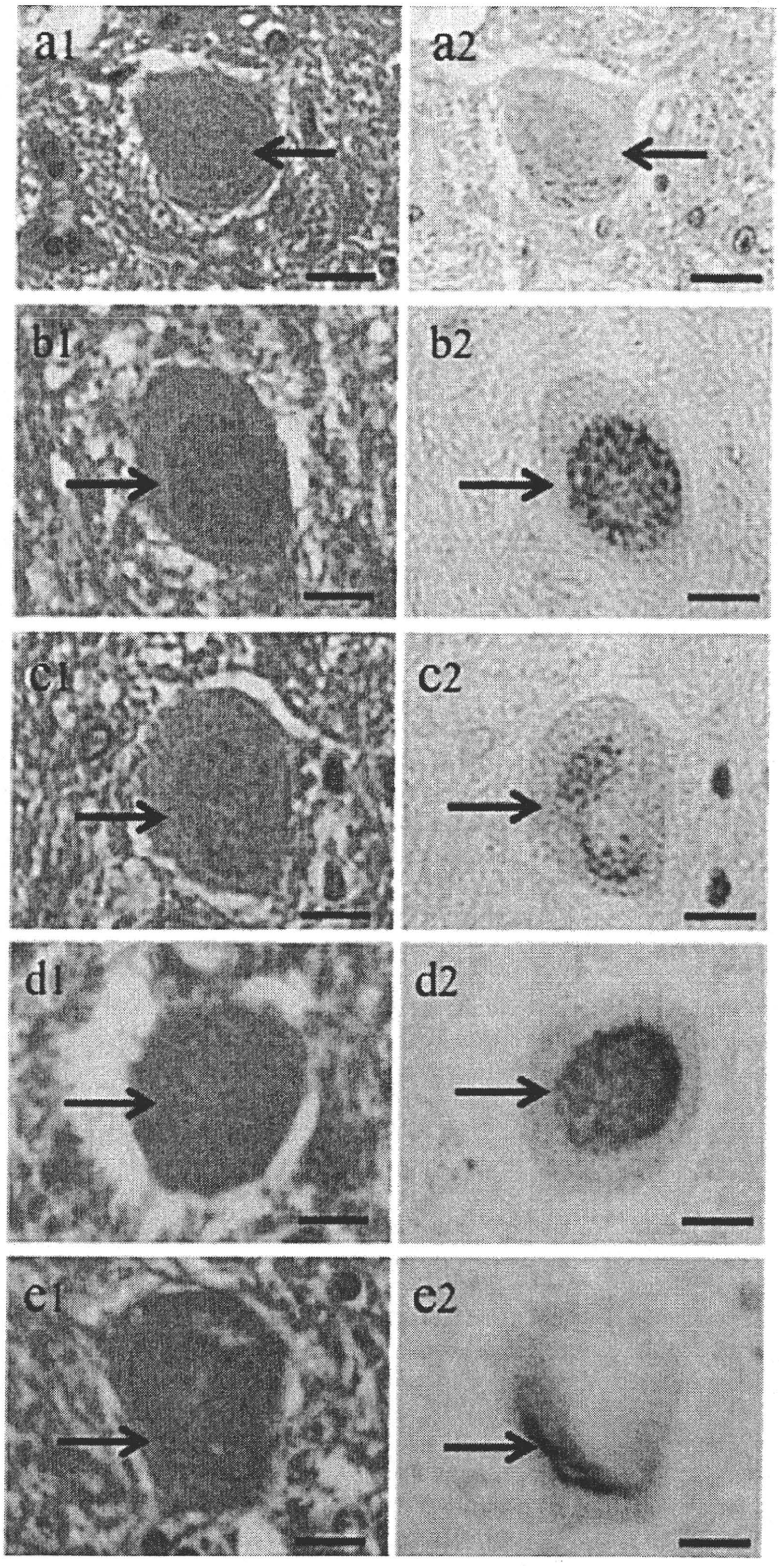

Fig. 1 Basophilic inclusions (BIs, indicated with arrows) in the anterior horn cells appear as round or globular basophilic masses after HE staining (a1–e1). BI was weakly argyrophilic with Gallyas-Braak stain (a2). BIs were strongly immunostained with anti-fused in sarcoma protein (FUS) (b2,c2) and anti-p62 (d2) antibodies in the same sections. Some BIs were labeled in only a part of the inclusion for anti-p62 antibody (e2). Scale bar: 20 μm.

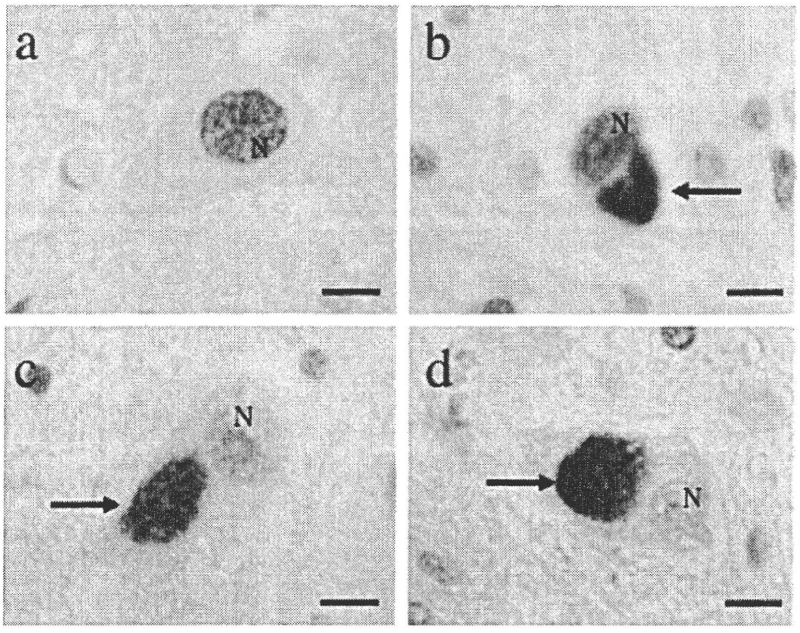

Fig. 2 Anti- fused in sarcoma protein (FUS) antibody immunostained the nucleus in a normal-looking anterior horn cell (a). Nuclear staining of FUS was preserved in an anterior horn cell containing a FUS-positive cytoplasmic inclusion (arrow) (b). Nuclear immunoreactivities of FUS were weak (c) or absent (d) in the anterior horn cells containing FUS-positive inclusions (arrows). N = nucleus, Scale bar: 20 μm.

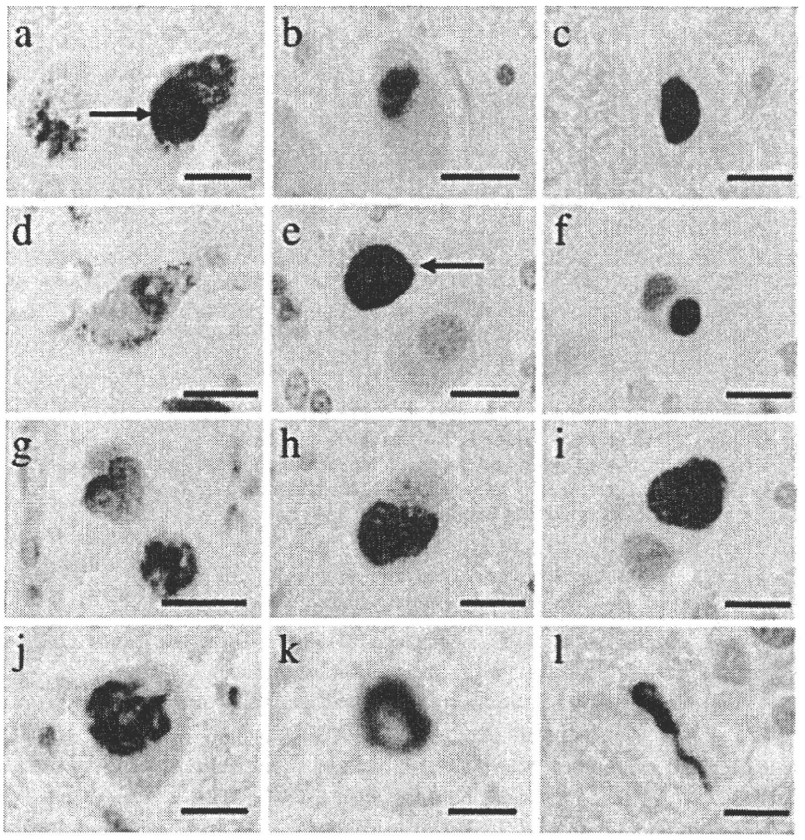

Fig. 3 Fused in sarcoma protein (FUS)-positive cytoplasmic inclusions are observed in the neurons of the substantia nigra (a, arrow), oculomotor nucleus (b), red nucleus (c), locus coeruleus (d), facial nucleus (e, arrow), pontine nucleus (f), inferior olivary nuclei (g), hypoglossal nucleus (h) and dentate nucleus (i). A FUS-positive skein-like cytoplasmic inclusion was seen in the anterior horn cell (j). A FUS-positive glial inclusion (k) and dystrophic neurite (l) were evident in the anterior horn. Scale bars: a–j, 20 μm; k, 5 μm; l, 15 μm.